

Performance impact of dynamic surface coatings on polymeric insulator-based dielectrophoretic particle separators

Rafael V. Davalos · Gregory J. McGraw ·
Thomas I. Wallow · Alfredo M. Morales ·
Karen L. Krafcik · Yolanda Fintschenko ·
Eric B. Cummings · Blake A. Simmons

Received: 10 April 2007 / Revised: 7 June 2007 / Accepted: 8 June 2007
© Springer-Verlag 2007

Abstract Efficient and robust particle separation and enrichment techniques are critical for a diverse range of lab-on-a-chip analytical devices including pathogen detection, sample preparation, high-throughput particle sorting, and biomedical diagnostics. Previously, using insulator-based dielectrophoresis (iDEP) in microfluidic glass devices, we demonstrated simultaneous particle separation and concentration of various biological organisms, polymer microbeads, and viruses. As an alternative to glass, we evaluate the performance of similar iDEP structures produced in polymer-based microfluidic devices. There are numerous processing and operational advantages that motivate our transition to polymers such as the availability of numerous innate chemical compositions for tailoring performance, mechanical robustness, economy of scale, and ease of thermoforming and mass manufacturing. The polymer chips we have evaluated are fabricated through an injection molding process of the commercially available cyclic olefin copolymer Zeonor 1060R. This publication is the first to demonstrate insulator-based dielectrophoretic biological particle differentiation in a polymeric device injection molded from a silicon master. The results

demonstrate that the polymer devices achieve the same performance metrics as glass devices. We also demonstrate an effective means of enhancing performance of these microsystems in terms of system power demand through the use of a dynamic surface coating. We demonstrate that the commercially available nonionic block copolymer surfactant, Pluronic F127, has a strong interaction with the cyclic olefin copolymer at very low concentrations, positively impacting performance by decreasing the electric field necessary to achieve particle trapping by an order of magnitude. The presence of this dynamic surface coating, therefore, lowers the power required to operate such devices and minimizes Joule heating. The results of this study demonstrate that iDEP polymeric microfluidic devices with surfactant coatings provide an affordable engineering strategy for selective particle enrichment and sorting.

Keywords Microfluidics/microfabrication · Surfactants · Biological samples · Bioanalytical methods

Introduction

To detect pathogens at low concentrations in typical lab-on-a-chip liquid samples, it is vital to develop selective techniques to collect, concentrate, and deliver particles of interest for testing and identification. Dielectrophoresis (DEP) has proven to be an effective means to manipulate such particles. DEP is the motion of particles driven by conduction effects in a nonuniform electric field [1]. It has been shown that DEP can be used to transport suspended particles utilizing either oscillating (AC) or steady (DC) electric fields [2]. DEP is suitable for differentiating

R. V. Davalos
School of Biomedical Engineering and Sciences,
Virginia Tech-Wake Forest University,
Blacksburg, VA 24061, USA

R. V. Davalos · G. J. McGraw · T. I. Wallow · A. M. Morales ·
K. L. Krafcik · Y. Fintschenko · E. B. Cummings ·
B. A. Simmons (✉)
Sandia National Laboratories,
7011 East Ave MS9292,
Livermore, CA 94551, USA
e-mail: basimmo@sandia.gov

biological particles (e.g., cells, spores, viruses, DNA) because it can collect specific types of particles rapidly and reversibly based on intrinsic properties including size, shape, conductivity, and polarizability [3].

Many device architectures and configurations have been developed to sort a broad range of biological particles by DEP. For example, early DEP experiments carried out by Pohl et al. utilized pin-plate and pin-pin electrodes to differentiate between live and dead yeast cells and collected them at the surface of the electrode [4, 5]. Currently, the typical dielectrophoretic device generates a nonuniform electric field using an array of thin-film interdigitated electrodes within a flow channel that interacts with particles near the surface of the electrode array [6]. The nonuniform electric fields are typically generated by a single-phase AC source, and in addition, multiple-phase sources can trap and sequentially transport particles in a technique called traveling-wave dielectrophoresis [7]. These electrode-based DEP devices are effective for separating and concentrating cells [8], proteins [9], DNA [10], and viruses [11].

Another approach is insulator-based dielectrophoresis (iDEP), which uses insulating obstacles, instead of electrodes, to produce spatial nonuniformities in an electric field that is applied through the suspending liquid. This iDEP technique was first presented by Masuda et al. [12] and subsequently developed further as a means of separating particles by Lee et al. [13]. It has been demonstrated, utilizing insulating glass structures and AC electric fields, that iDEP can separate DNA molecules, *Escherichia coli* cells, and red blood cells [14]. Similarly, Zhou et al. [15] and Suehiro et al. [16] used channels filled with insulating glass beads and applied AC electric fields to separate and concentrate yeast cells in water. Benguigui and Lin have also demonstrated the dielectrophoretic separation of various particles in nonconductive liquids using a similar technique [17]. We expanded these findings to microfluidics developing glass-based iDEP devices with a DC electric field applied across an array of insulating posts inside the microfluidic channel. Examples include trapping of polystyrene particles [18], separating live from dead bacteria [19], differentiating live species of bacterial prokaryotic cells [20], and the trapping and concentration of viruses [21]. We have also demonstrated that ridge-based architectures can be used in addition to post-based architectures [22–24]. While glass-based iDEP microdevices perform well, devices are expensive and sample throughput is low because of the geometrical limitations of isotropically etched devices [25].

The present study demonstrates the capabilities and increased flexibility of polymer-based iDEP devices and explores the possibility of performance enhancement through the use of a dynamic coating. Previously, we demonstrated using a glass master that iDEP elements can

be made from a cyclic olefin copolymer, Zeonor [25]. Cyclic olefin copolymers have received a significant amount of interest in microfluidics owing to their low auto-fluorescence and high chemical resistance to a large range of polar solvents [26, 27]. In recent years, polymer-based microfluidic devices have been developed for many lab-on-a-chip applications. Among them are liquid/liquid sorting, particle separation, capillary electrophoresis, miniaturized polymerase chain reaction (PCR) chambers, nucleic acid analysis, protein analysis, and fluidic mixers [28–30]. The main appeal of these polymeric devices is that they are relatively inexpensive, employing standard mass fabrication techniques such as injection molding and hot embossing instead of microlithography [31, 32].

The polymer-based iDEP devices in this study are injection molded using a nickel stamp electroplated on a straight-walled anisotropically etched silicon master. Unlike isotropically etched channels in glass masters, the deep prismatic channels in an anisotropic silicon master allow for a high volumetric flow rate. The DEP behavior of the particles (both biological and inert) was observed to be a function of the magnitude of the applied DC electric field and the characteristics of the particle such as size, shape, and conductivity. This study presents the first demonstration of insulator-based dielectrophoretic biological particle differentiation in a polymeric device injection molded using a silicon master. Additionally, we demonstrate that by using surfactants, we discover a new flexibility to meet a wide range of operational requirements. It has been previously shown that other additives, such as hydroxypropylmethylcellulose, are an effective method of suppressing electroosmotic flow in microfluidic devices fabricated with Zeonor [32]. The utilization of surfactants as dynamic coatings has been widely investigated in capillary electrophoresis [33] and microfluidic applications [34]. We present a quantitative determination of the interaction between the hydrophobic Zeonor 1060R polymer surface and the nonionic block copolymer surfactant, Pluronic F127, as a function of concentration through quartz crystal microbalance (QCM) studies. The presence of the nonionic surfactant at very low concentrations in the solution produces a fully saturated surfactant coating on the polymer. This coating results in a significant, almost tenfold, reduction in the magnitude of the applied electric field necessary to trap inert beads. Lowering the field lowers the power required to operate such devices, which minimizes the Joule heating present and increases the operational stability of the iDEP device. In summary, the polymeric devices exhibit the same characteristic DEP behavior of glass devices, but with higher throughput (milliliters per hour), ease of mass fabrication, the ability to support a variety of scalable physical formats, and the flexibility of surfactants as dynamic coatings to meet a diverse range of operational requirements.

Theory

Dielectrophoresis is defined as the motion of a particle due to its polarization induced by the presence of a nonuniform electric field. The DEP force acting on a spherical particle can be described by the following [35, 36]:

$$F_{DEP} = 2\pi\epsilon_0\epsilon_m r^3 \operatorname{Re}\{f(\tilde{\sigma}_p, \tilde{\sigma}_m)\} \nabla E^2 \quad (1)$$

where ϵ_0 is the permittivity of free space, ϵ_m is the relative permittivity of the suspending medium, r is the radius of the particle, ∇E^2 defines the local gradient of the electric field, $\tilde{\sigma}_p$ and $\tilde{\sigma}_m$ are the complex conductivities of the particle and the medium respectively, and $f(\tilde{\sigma}_p, \tilde{\sigma}_m)$ is defined as the Clausius–Mossotti factor:

$$f(\tilde{\sigma}_p, \tilde{\sigma}_m) = (\tilde{\sigma}_p - \tilde{\sigma}_m) / (\tilde{\sigma}_p + 2\tilde{\sigma}_m) \quad (2)$$

Equations (1) and (2) indicate that the dielectrophoretic force acting on a particle can be positive or negative in magnitude. For frequencies below 100 kHz, the real currents typically dominate the displacement currents and the Clausius–Mossotti factor can be approximated in terms of the real conductivities (i.e., $\tilde{\sigma}_i \approx \sigma_i$). In this scenario, if the conductivity of the particle is greater than the conductivity of the medium, then the particle will exhibit positive DEP behavior and move toward regions of high electric field. If, as is typical for biological particles, the particle is less conductive than the suspending medium, the particle exhibits negative DEP and moves away from regions of high electric field. Since we primarily use DC

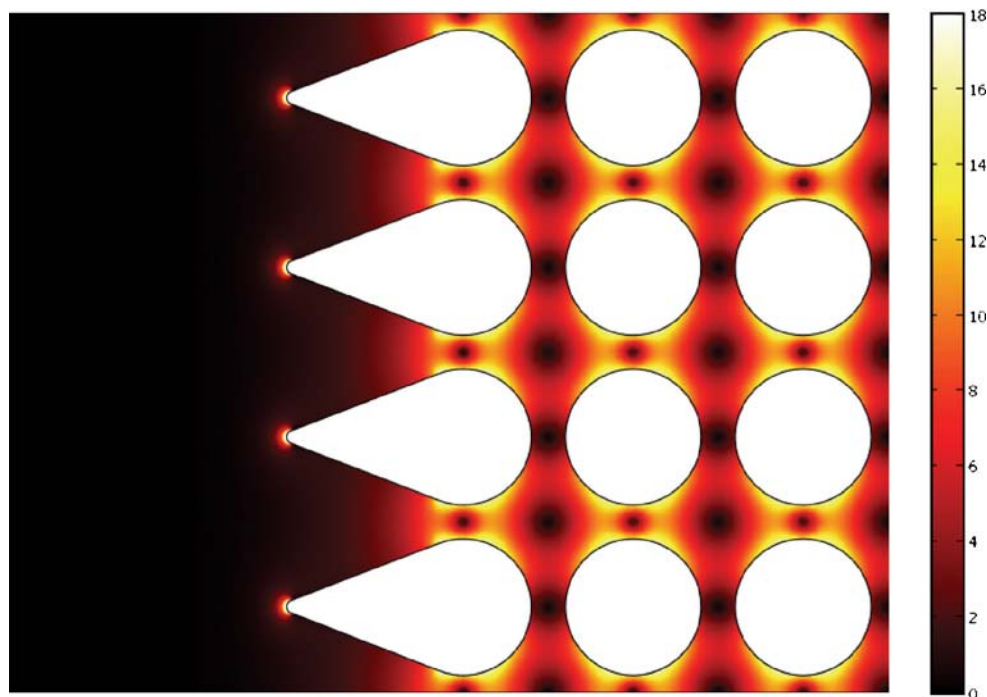
electric fields in our devices, the dielectrophoretic force exerted on the particles for a given electric field gradient depends only on the conductivity of the particle, the conductivity of the medium, and the size of the particle.

For a particle to become trapped in our device, the dielectrophoretic force on the particle must overcome the electrokinetic force on the particle [20]. This can be represented mathematically as:

$$\frac{u_{DEP} \cdot u_{EK}}{u_{EK} \cdot u_{EK}} = \frac{\mu_{DEP}}{\mu_{EK}} \frac{\nabla(E \cdot E)}{E \cdot E} \cdot E > 1 \quad (3)$$

where $u_{DEP} = \mu_{DEP} \nabla(E \cdot E)$ and μ_{DEP} are the dielectrophoretic velocity and mobility of the particle, respectively, and $u_{EK} = \mu_{EK} E$ and μ_{EK} are the electrokinetic velocity and mobility of the particle. As the field strength is increased, dielectrophoresis increases as the square of the field and electrokinetic flow only increases linearly with the field. As depicted in Eq. (3), eventually the dielectrophoretic velocity overcomes the electrokinetic velocity and the particles trap. It has been previously demonstrated by some of the co-authors that for particles greater than 500 nm in diameter, the most effective geometry of the insulating structures for efficient particle separation are those of spherical cylinders (posts) arranged in an orthogonal array [18–21]. Figure 1 presents a simulation using COMSOL (COMSOL, Inc., Burlington, MA) depicting the ratio of the electric field gradient to the local electric field, normalized by the applied field and the post diameter that occurs as a result of this insulating array structure.

Fig. 1 Simulation depicting the ratio of the electric field gradient to the local electric field, normalized by the post diameter (d) over the applied field (V/L), within the insulating structure array of the iDEP device. (i.e., $(dL/V) \nabla(E \cdot E)/E$)



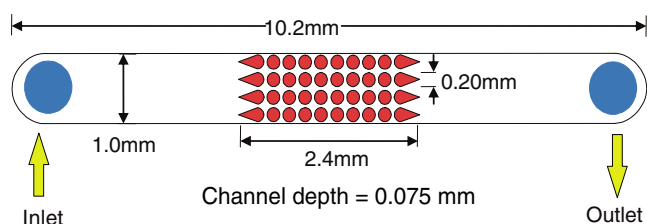


Fig. 2 Schematic depiction of the typical experimental device configuration used in iDEP studies showing the arrays of insulating posts in the middle of the channel and the fluidic reservoirs in which the electrodes are placed

Experimental

Chemicals

Deionized (DI) water from a reverse osmosis filter was titrated with NaOH and HCl to a pH of approximately 8. Conductivity was then adjusted by titration with KCl to an endpoint of 2–4 $\mu\text{S}/\text{cm}$. Carboxylate (green) and/or rhodamine (red) surface-modified polystyrene microspheres, FluoSpheres, (Molecular Probes, Eugene, OR) having a density of 1.05 mg/mm^3 and of various sizes were diluted 1:1,000,000 in the background solution from a 2 wt.% stock suspension. Bead suspensions were stored in a refrigerator and sonicated between dilution steps and before use. The bead suspensions were filtered using an appropriate pore size syringe filter to remove larger bead aggregates before use.

Labeling of biological organisms

Bacillus thuringiensis and *Bacillus subtilis* spore suspensions were obtained from Raven Biological Laboratories Inc. (Omaha, NE). The unmodified spore samples were then labeled with Syto 17 (red) dye (Molecular Probes, Inc., Eugene, OR). For every milliliter of spore sample present in the vial, 3 μL of the fluorescent nucleic acid stain was added. The solution was then incubated at room temperature for 10 min. The labeled spores were recovered by centrifugation at 14,000 rpm for 10 min, washed three times with DI water to remove any excess dye, and re-suspended in DI water to reach the desired concentration

(typically 1×10^9 spores/mL). The labeled spore solutions were then diluted between 1:20 and 1:100 by volume in pH and conductivity controlled deionized water. Approximately 20 μL of diluted sample was added to the inlet reservoir of the flow manifold via pipette.

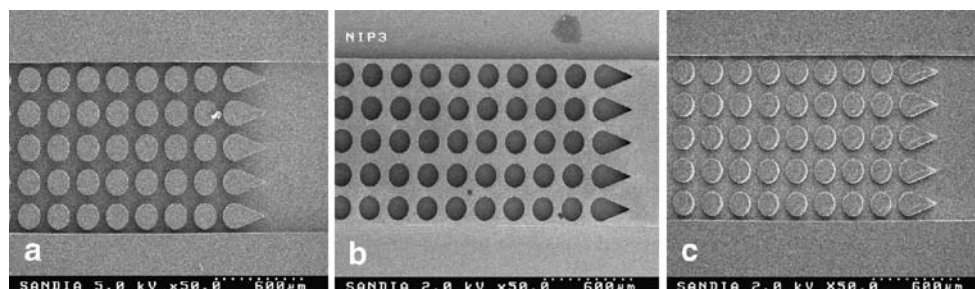
iDEP microfluidic design

A schematic of a microchannel can be seen in Fig. 2. Each microchannel is 1 mm wide, and 10.2 mm end-to-end, with a nominal depth of 75 μm . Towards the middle of the microchannel is an array of insulating posts arranged in ten sequential columns of four. These circular posts are 200 μm in diameter, are spaced 250 μm center-to-center, and traverse the entire depth of the channel. The posts of the front and back columns have the same width and spacing, but taper outward to reduce fouling.

Replication tool

A custom stamp with a negative of the microchannel troughs and posts on its surface was used to injection mold the polymeric microfluidic devices. The stamp was fabricated using a silicon master with features for eight independent microchannels photolithographically etched into its surface. A two-step anisotropic etch process was employed to produce features for eight independent microchannels with straight sidewalls to a depth of 75 μm on the Si master (Fig. 3a). After patterning, the masters were sputter coated with an electroplating base material, in this case 500 \AA of chrome (for adhesion promotion) and 1,500 \AA of copper. The masters were then placed into a Digital Matrix commercial DM3M electroplating machine. The bath chemistry utilized was a standard nickel sulfamate with controlled pH, typically around 4, to minimize stresses. Electroplating occurred at 48 $^\circ\text{C}$ for a total of 40 Ah and produced nickel films with thickness typically on the order of 1 mm. The electroplated nickel stamp was then planarized and machined to the set dimensions for use in our custom in-house fabrication facilities and released from the master. The nickel stamp (Fig. 3b) was then thoroughly characterized through metrology, visual inspec-

Fig. 3 Images depicting the fabrication route of a polymer-based iDEP device from the **a** initial silicon features to **b** electroformed nickel stamp and finally to **c** injection molded polymer replicate



tion, and electron microscopy. Since the stamp is a negative of the master, the master and the final polymer disc contain the same features (Fig. 3c).

Polymer replication

Polymeric discs were injection molded from Zeonor 1060 resin (Zeon Corp., Tokyo, Japan) using the custom stamp containing the negative of the eight independent microchannels (Fig. 3b). Injection molding was carried out utilizing a 60-ton Nissei TH-60 vertical injection molding machine (Nissei America, Los Angeles, CA). Pellets of Zeonor 1060R resin (Zeon Chemicals, Louisville, KY) were dried at 40 °C for at least 24 h before use. The resin was then fed to the machine through a gravity-assisted hopper connected externally to the injection molding barrel. Device operators empirically optimized the operational conditions using a starting point recommended by the resin supplier. Cross-polarized optical interrogation of the replicated substrates was employed to assess and minimize residual stresses in the injection molded parts. The resulting Zeonor microchannel is shown in Fig. 3c.

Premanufactured 1.6-mm-thick discs of Zeonor 1060R from Zeon Chemicals (Louisville, KY) were used as lids to seal the channels. Vias of 1-mm diameter were drilled through the discs using a Uniline-2000 drill (Excellon Automation Co., Rancho Dominguez, CA) to provide a fluidic interface at each end of the eight microchannels. The holes are located at either end of the channel, approximately 2.9 mm from the array of posts.

The discs containing the microfluidic channels were then thermally bonded to discs containing the vias using a Carver press (Carver, Inc., Wabash, IN). Bonding conditions were held constant at the following: the press was heated to 190 °F with a constant applied load of 750 psig and a corresponding cycle time at temperature of 60 min. The bonded assembly was then cooled to 75 °F under constant load and then removed from the press. All bonded assemblies were checked for flow and channel blockage before use.

Experimental setup

The bonded disc was reversibly sealed to the base of a custom PDMS manifold using a vacuum chuck. The manifold is ported with 16 openings spanning its thickness that coincide with the inlet and outlet vias of each channel. Each opening can accept a slip tip syringe and forms a watertight seal with the syringe and a drilled via in the lid. The channels were primed by gently forcing background solution through the channel. A programmable high voltage sequencer, Labsmith HVS 448 (Livermore, CA) was used to apply voltages of up to 1,500 V. A manually controlled power supply, Bertran ARB 30 (Valhalla, NY) was used for

higher voltages. Data was collected with an inverted epifluorescence microscope, Olympus model IX-70 (Olympus, Napa, CA), equipped with an Optonics digital camera (Optonics, Goleta, CA) and an appropriate fluorescence filter set.

Concentration factor measurement

After the bead suspensions were introduced into the device, the liquid level in the syringes was balanced to ensure quiescent flow. To calculate the baseline concentration of particles, the flow of the tracer suspension through an unobstructed region of the channel was recorded with the camera for 30 to 60 s. These baseline measurements were taken with an applied DC voltage of 200 V, which is sufficient to produce a steady electroosmotic flow, but well below the iDEP trapping threshold. After the baseline data was acquired, DC voltage was increased to the specified trapping voltage. During this period, iDEP trapping around the posts could be clearly observed. Once the trapping voltage had been applied for the specified time, the voltage was discontinued, and trapped particles were allowed to flow to the front of the posts under the backpressure generated by electroosmotic flow during the trapping run. This release plug was filmed for later counting.

The maximum concentration of particles was determined by a manual count of the frame of the release plug video in which the plug is most dense. The concentration factor, CF, represents the ratio of the maximum observed concentration of beads in the plug to the average concentration observed in the baseline video. This was calculated with the formula:

$$CF = \frac{1}{L} \frac{N_p f}{N_b \tau} \quad (4)$$

where L is the length of the plug as a fraction of the total frame length, N_p and N_b are the maximum count of beads in the release plug and the bead count for the entire baseline video segment, respectively. τ is the period required for a flowing particle in the baseline video to cross the frame length given in frames, and f is the total duration of the baseline video given in frames.

Quartz crystal microbalance

Interactions of Zeonor 1060R films with surfactant solutions were studied using a modified commercially available compensated phase-locked oscillator (CPLO)-equipped quartz crystal microbalance (QCM) (RQCM, Maxtek Corporation, Cypress, CA). The CPLO is used along with extensions of standard QCM physical models to help resolve difficulties associated with films and to facilitate analysis. Zeonor films were prepared by dissolving injection-molded Zeonor 1060R stock in cineole. Thin films were spin cast at

1,500 rpm on gold-electrode coated AT-cut quartz crystals with nominal fundamental resonant frequencies of 5 MHz. Following coating, the Zeonor films ($0.325 \pm 0.005 \mu\text{m}$ thickness) were baked in air at $180 \text{ }^\circ\text{C}$ for 10 min. Film thickness characterization of witness pieces by profilometry and interferometry indicated that highly reproducible, striation-free films are produced under the spin-casting conditions employed. Coated wafers were then mounted in immersion holders. Covered glass containers filled with doubly deionized water were placed in a thermostatted bath at $25 \pm 0.1 \text{ }^\circ\text{C}$ and allowed to equilibrate for several hours. Surfactant samples from a 0.25 wt.% stock solution were introduced at set time intervals and measurements were taken as a function of the response to the increased surfactant concentration. Solutions were stirred using a Teflon-coated stir bar. The concentrations studied ranged from 1×10^{-7} to $1 \times 10^{-1} \text{ M}$.

Results and discussion

Differential trapping of various particle types

The first step in comparing the performance of the polymer devices to that of glass is to evaluate how well the system performs at selectively separating and removing fluorescent-polystyrene beads, which we employ as a surrogate background. As indicated by zeta potential measurements of Zeonor [32], stable electrokinesis of particles toward the negative electrode is observed at low field strengths. As the field strength is increased, dielectrophoresis increases as the square of the field according to Eq. (1). Electrokinetic flow, which increases linearly with the field, is overcome and the polystyrene beads are observed to trap between the posts at an applied voltage of 300 V as shown in the image in Fig. 4a. The value of the applied electric field when the dielectrophoretic force dominates the electrokinetic force is, therefore, termed the trapping threshold. This trapping of particles is reversible, and the beads are released from the traps when the electric field is decreased below the trapping threshold. In addition to being able to trap a certain size of bead, differential trapping based on bead size was shown. Two sizes of fluorescently labeled polystyrene beads were mixed together to form a suspension of 1- μm green and 2- μm red beads. Figure 4b shows differential trapping of the beads at an applied voltage of 1,000 V, as indicated by the formation of localized regions of red and green beads between the posts. This result demonstrates the capability of the polymer-based iDEP devices to trap and differentiate particles based on size in a manner equivalent to that observed in the glass microdevices.

The next area of research was to assess whether polymeric iDEP microdevices are capable of separating

and concentrating suspensions of mixed biological and inert particles. The results for *Bacillus thuringiensis* spores mixed with 1- μm fluorescent beads at an applied voltage of 720 V are presented in Fig. 4c. As the applied DC electric field is increased in magnitude, a transition is observed from unimpeded spore movement at lower field strengths to well-developed trapping of the spores at higher field strengths. Since the beads continue to travel between the posts as the spores are collected, the result shows how particles of different dielectrophoretic mobilities can be separated. As the field is increased, we can achieve trapping of the spores and beads as well as a banding and separation effect within the trapping region. Figure 4d is obtained with *Bacillus subtilis* spores mixed with 20-nm fluorescent beads with an applied voltage of 2,800 V. This voltage is much higher than the corresponding trapping threshold voltage for this spore species and demonstrates that the devices are stable over a large range of applied field strengths. The results in Fig. 4 demonstrate that for a given DEP mobility, the operation of the polymer iDEP devices can be tailored to effectively separate and enrich a given particle against a diverse background using an equivalent low-pass filter technique that can be staged to deliver a relatively monodisperse sample.

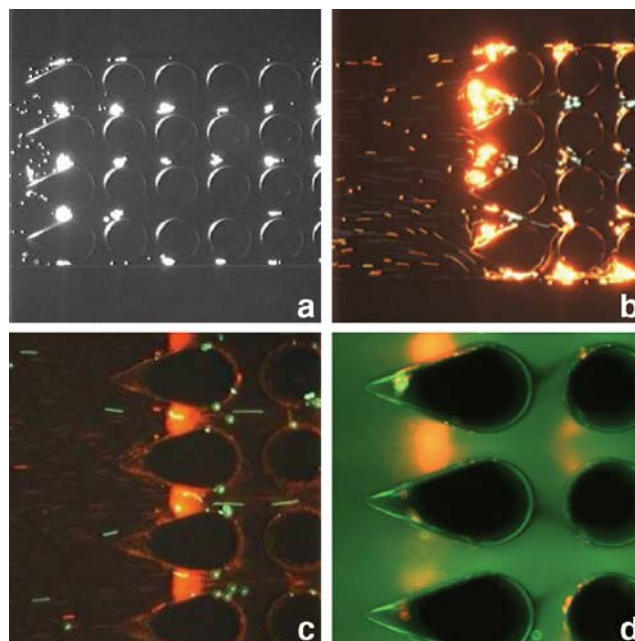


Fig. 4 Images obtained from digital movies taken of **a** trapping of 2- μm fluorescent polystyrene beads using an applied voltage of 300 V, **b** differential trapping of 1- μm green and 2- μm red beads at 1,000 V, **c** trapping of *Bacillus thuringiensis* spores (red) in the presence of 1- μm beads (green) using an applied voltage of 720 V, and **d** separation of *Bacillus subtilis* spores (red) from 20-nm beads (green) at 2,800 V. The net particle motion in all images is from left to right. Posts are 200 μm in diameter with a 250- μm center-to-center spacing in **a** and **b**, and 150 μm in diameter with 200- μm center-to-center spacing in **c** and **d**

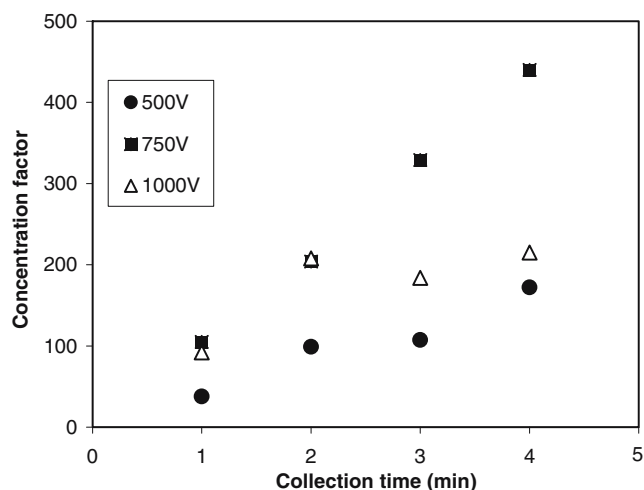


Fig. 5 Concentration factor of particles as a function of collection time and voltage

Baseline device performance

The performance of polymeric iDEP devices was quantified to compare it to that of glass microfluidic devices reported previously [21]. Figure 5 shows the concentration factor of polystyrene beads as a function of voltage and collection time. At 500 V and 750 V, the concentration factor increases with time as expected. At 1,000 V, there is a decrease in the concentration factor after approximately 3 min. The decrease in the concentration factor occurs when the traps in the first two post arrays saturate. As the traps saturate, particles spill down and are collected in subsequent traps, which broadens the concentration plug (i.e., L in Eq. (4) increases). The traps saturate more rapidly at 1,000 V because the particles are driven electrokinetically at

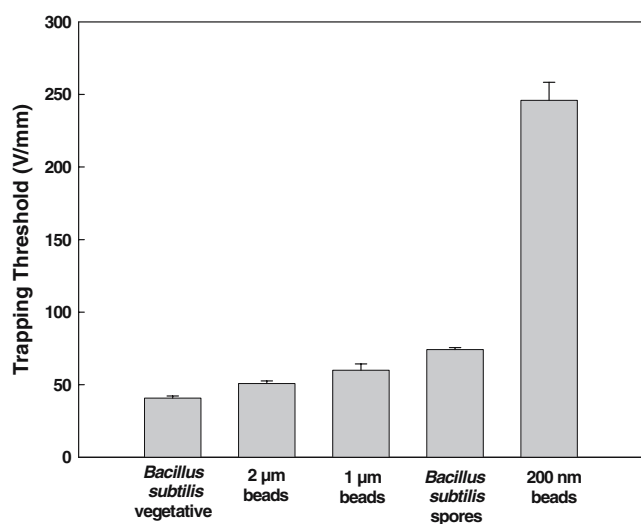


Fig. 6 Summary of the different magnitudes of the applied DC electric fields required to trap, defined here as the trapping threshold (y -axis), a variety of different inert and biological particle types ($n=5$)

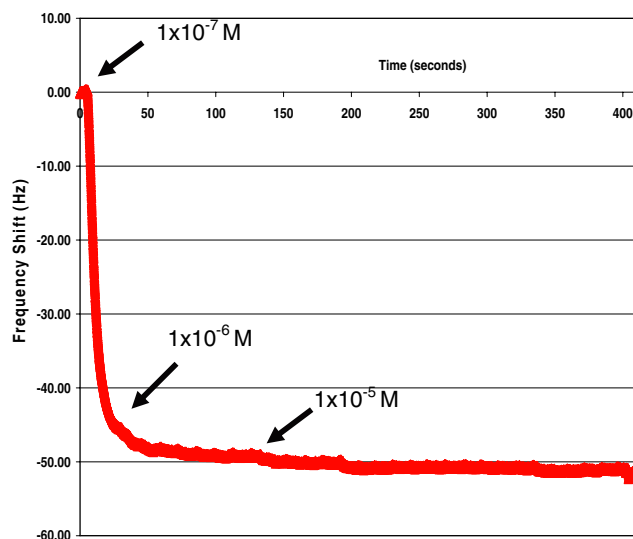


Fig. 7 Plot of frequency shift of the QCM device as a function of time and Pluronic F127 concentration on a Zeonor 1060R film

a faster rate. The preliminary results in Fig. 4 illustrate that concentration factors on the order of several hundred are attainable using our prescribed conditions.

A summary of the trapping thresholds observed for a variety of biological and inert particle types for the Zeonor iDEP devices is presented in Fig. 6. We observe the typical dependence on both particle size and type as that reported previously for glass iDEP microdevices and with comparable results [21]. For example, in the case of *Bacillus subtilis* vegetative cells, the trapping threshold in the glass devices is 48.1 ± 2.3 V/mm, whereas for the Zeonor devices it is 40.8 ± 1.4 V/mm. The lower trapping threshold in Zeonor is expected as the zeta potential of the glass is higher than that of Zeonor [32] and, therefore, the glass produces a higher

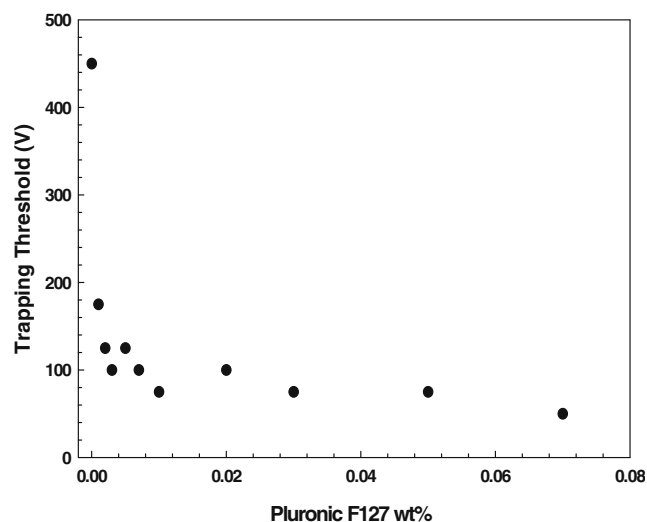


Fig. 8 Plot of threshold trapping voltages for 2-μm carboxylate modified FluoSpheres in the presence of an electroosmotic flow as a function of Pluronic F127 weight%

electrokinetic force on the particle that must be overcome before trapping. The experimental results in Figs. 4 and 6 agree with the iDEP theory [18] and illustrate the effectiveness of these devices in separating targeted waterborne biological particles from background particles.

Impact of nonionic dynamic surface coatings

The results from the QCM experiments monitoring surfactant adsorption are presented in Fig. 7 and demonstrate the temporal and concentration dependence of the Pluronic F127 adsorption onto the Zeonor 1060R thin film. As the surfactant is adsorbed onto the Zeonor thin film it produces a negative frequency shift on the QCM crystal. This negative shift observed in the frequency response of the crystal is therefore directly proportional to the amount of surfactant that adsorbs onto the surface of the polymer. It can be clearly seen from the data that the surfactant forms a saturated layer onto the Zeonor 1060R surface at low concentrations of approximately 10 μM . This concentration is much lower than the commonly reported values of the critical micelle concentration of the surfactant at this temperature [37]. Using the data obtained from the frequency shift plots, we have calculated that the F127 coating on the polymer film has a mass of about 8.4×10^{-12} ng/nm² and represents 0.4 F127 molecules per nm² on the polymer surface. It is known that the presence of this adsorbed surfactant layer on a polymer surface can effectively disrupt the electroosmotic flow present for a given solution by mitigating the surface charge migration that occurs in an electroosmotic flow condition [38].

Figure 8 depicts the trapping voltages for 2- μm carboxylate modified latex beads in the presence of an electroosmotic flow as a function of surfactant concentration. Separate measurements taken on the electrophoretic mobility of the polystyrene beads as a function of surfactant concentration demonstrated that the effect of the surfactant was minimal as compared to the effect of the surfactants on the electroosmotic flow. Our results show that the trapping threshold decreases with increasing surfactant concentration, reinforcing our hypothesis that the presence of the surfactant is disrupting the electroosmotic flow velocity and thereby lowering the effective electrokinetic force of the system. This lowers by a factor of 9 the applied electric field in which the dielectrophoretic force term becomes dominant in the overall force balance felt on the particle and becomes trapped. The use of surfactants lowers the power required to operate such devices, which minimizes the Joule heating present and increases the operational stability of the iDEP device. These results suggest that the nonionic block copolymers can be employed at very low concentrations in order to greatly improve the performance of the polymer iDEP device while simultaneously maintaining good solution and sample

characteristics. We will conduct further work into other types of ionic and nonionic surfactants, as well as photografting techniques, to develop a robust matrix of potential surface modifications and their impact on iDEP performance.

Conclusions

We have demonstrated that polymer-based iDEP devices are effective for the selective trapping and concentration of a range of biological and inert particles in an aqueous sample. A nonuniform electric field was generated by applying a DC electric field across a polymeric microchannel containing insulating posts. Regions of high field intensity generated between these posts selectively repelled particles dielectrophoretically, producing selective and field-tunable particle traps for a broad range of particle types. The performance of the polymer-based iDEP microdevices at removing and concentrating particles selectively is similar to that obtained in the glass-based iDEP microdevices. We also found that the surfactant Pluronic F127 interacts strongly with the hydrophobic polymer surface. The presence of dilute amounts of these surfactants greatly reduces the electric fields required to trap particles via dynamic surface coating of the polymer channel. This approach shows promise for numerous other surface modifications, both dynamic and static, in order to improve iDEP device performance depending on the application. These results illustrate the great potential of polymer-based iDEP devices for the concentration and sorting of a wide variety of biological and nonbiological particles. We envision a role for polymeric iDEP devices in front-end sample preparation to enhance bacterial analysis and detection in any lab-on-a-chip integrated detection system.

Acknowledgments This work was performed by Sandia National Laboratories for the United States Department of Energy under Contract DE-AC04-04AL85000. This project was funded by the Laboratory Directed Research and Development Program of Sandia National Laboratories. The authors thank John Hachman, Renee Shediak, Mike Firreno, Cindy Hamett, Marion Hunter, Brian Holliday, John Brazzle, Judith Rognlien, George Sartor, Blanca Lapizco-Encinas, and Linda Domeier for their assistance in every phase of this project.

References

1. Pohl H (1951) *Appl Phys* 22:869–871
2. Pohl H (1958) *Appl Phys* 29:1182–1188
3. Gascoyne P, Vykoukal J (2002) *Electrophoresis* 23:1973–1983
4. Pohl H, Hawk I (1966) *Science* 152:647–649
5. Crane J, Pohl H (1968) *J Electrochem Soc* 115:584–586
6. Yang J, Huang Y, Wang X, Becker F, Gascoyne P (1999) *Anal Chem* 71:911–918

7. Hughes M, Pethig R, Wang X-B (1996) *J Phys D Appl Phys* 29:474–482
8. Markx GH, Huang Y, Zhou XF, Pethig R (1994) *Microbiology* 140:585–591
9. Zheng L, Brody JP, Burke PJ (2004) *Biosens Bioelectron* 20:606
10. Washizu M, Kurosawa O (1990) *IEEE Trans Ind Appl* 26:1165–1171
11. Akin D, Li H, Bashir R (2004) *Nano Lett* 4:257–259
12. Masuda S, Itagaki T, Kosakada M (1988) *IEEE Trans Ind Appl* 24:740–744
13. Lee S-W, Yang S-D, Kim Y-W, Kim Y-K, Lee S-H (1994) *Conference of IEEE Engineering in Medicine and Biology Society*, pp 1019–1020
14. Chou C, Tegenfeldt J, Bakajin O, Chan S, Cox E, Darnton N, Duke T, Austin R (2002) *Biophys J* 83:2170–2179
15. Zhou G, Imamura M, Suehiro J, Hara M (2002) 37th annual meeting of the IEEE Industry Applications Society, Pittsburgh, Pennsylvania
16. Suehiro J, Noutomi D, Shutou M, Hara M (2003) *J Electrostatics* 58:229–246
17. Benguigui L, Lin IJ (1982) *Sep Sci Technol* 17(8):1003–1017
18. Cummings EB, Singh A (2003) *Anal Chem* 75:4724–4731
19. Lapizco-Encinas BH, Simmons BA, Cummings EB, Fintschenko Y (2004) *Anal Chem* 76:1571–1579
20. Lapizco-Encinas BH, Simmons BA, Cummings EB, Fintschenko Y (2004) *Electrophoresis* 25:1695–1704
21. Lapizco-Encinas BH, Davalos RV, Simmons BA, Cummings EB, Fintschenko Y (2005) *J Microbiol Methods* 62:317–326
22. Davalos RV, Lapizco-Encinas BH, Fiechtner GJ, Singh AK, Simmons BA, Fintschenko Y, Cummings EB (2004) *MicroTAS 2004*, Malmo, Sweden
23. Barrett LM, Skulan AJ, Singh AK, Cummings EB, Fiechtner GJ (2005) *Anal Chem* 77:6798–6804
24. Skulan AJ, Barrett LM, Singh AK, Cummings EB, Fiechtner GJ (2005) *Anal Chem* 77:6790–6797
25. McGraw GJ, Davalos RV, Brazzle JD, Hachman JT, Hunter MC, Chames JM, Fiechtner GJ, Cummings EB, Fintschenko Y, Simmons BA (2005) *SPIE proceedings: MOEMS-MEMS 2005 - micromachining and microfabrication process technology X*, San Jose, CA
26. McGraw GJ, Davalos RV, Cummings EB, Fintschenko Y, Fiechtner GJ, Simmons BA (2005) *Polym Prepr (Am Chem Soc Div Polym Chem)* 46:1208
27. McGraw GJ, Davalos RV, Mittal BM, Ferko SM, Hunter MC, Brazzle JD, Fintschenko Y, Cummings EB, Simmons BA (2005) 9th international conference on miniaturized systems for chemistry and life sciences, Boston, MA
28. Wainright A, Nguyen UT, Bjornson T, Boone TD (2003) *Electrophoresis* 21:3784–3792
29. Fiorini GS, Chiu DT (2005) *BioTechniques* 38
30. Becker H, Gartner C (2000) *Electrophoresis* 21:12–26
31. Becker H, Locascio LE (2002) *Talanta* 56:267–287
32. Mela P, Van Den Berg A, Fintschenko Y, Cummings EB, Simmons BA, Kirby BJ (2005) *Electrophoresis* 26:1792–1800
33. Baryla NE, Melanson JE, McDermott MT, Lucy CA (2001) *Anal Chem* 73:4558–4564
34. Wang A-J, Xu J-J, Chen H-Y (2003) *Anal Chim Acta* 569:188–194
35. Pohl H (1978) *Dielectrophoresis*. Cambridge University Press, Cambridge
36. Jones TB (1995) *Electromechanics of particles*. Cambridge University Press, USA
37. Desai PR, Jain NJ, Sharma RK, Bahadur P (2001) *Colloids Surf A: Physicochem Eng Aspects* 178:57–69
38. Gaudio J, Craighead HG (2002) *J Chromatogr A* 971:249–253